



NLR-TP-2000-520

Technology for conformal load-bearing antennas on aircraft structures

J. Verpoorte, H. Schippers and G. Vos



NLR-TP-2000-520

Technology for conformal load-bearing antennas on aircraft structures

J. Verpoorte, H. Schippers and G. Vos

This report is based on a presentation held on the symposium “Antennas for Earth Observation”, at the Technical University of Delft on 8 and 9 June 2000.

The contents of this report may be cited on condition that full credit is given to NLR and the authors.

Division:	Avionics
Issued:	October 2000
Classification of title:	Unclassified



Contents

INTRODUCTION	3
THE CLAAS PROJECT	3
AIRCRAFT DYNAMICS	4
Elasto-mechanical modelling	4
Unsteady aerodynamic analysis	4
Computation of dynamic deformations	4
Electro-magnetic modelling	5
Numerical approach	6
EXAMPLE OF AN AIRBORNE CONFORMAL ANTENNA	6
EXAMPLE OF A SPACEBORNE CONFORMAL ANTENNA	7
POTENTIAL MEASURES TO REDUCE DEFORMATION AND VIBRATION EFFECTS	7
CONCLUSIONS	7
REFERENCES	7

15 Figures

(10 pages in total)

INTRODUCTION

The use of *conformal antennas* on aircraft allows the choice of non-conventional antenna locations such as the skin of the aircraft. However, when antennas are installed at these locations on the aircraft, they are subject to steady and unsteady aerodynamic loads. The inertial forces and these aerodynamical loads will cause *deformations* and *vibrations* of the total antenna surface. The effect of these deformations and vibrations on the antenna performance will be most significant on (highly) directional antennas. On aircraft, antennas with high directivity are mostly used for high frequency applications (>1 GHz). One of these applications is earth observation. Remote sensing of the earth is carried out by optical sensors and by Synthetic Aperture Radars (SAR). Synthetic Aperture Radars are employed on both spacecraft and aircraft for earth observation. On aircraft, the use of conformal array antennas for the application of SAR is very challenging. However, any change in main beam direction, beamwidth and/or side lobe level due to vibrations and deformation, will have an effect on the synthetic aperture and thus on the final image produced by the SAR.

THE CLAAS PROJECT

In order to assess the effects of surface vibrations and deformations on the performance of conformal antennas on aircraft, NLR carries out a National Technology project (under contract to the Netherlands Ministry of Defence) with the title: Conformal Load-bearing Antennas on Aircraft Structures (acronym CLAAS). This technology development requires contributions from the following research disciplines:

- Aerodynamic research: to provide knowledge about the size of steady and unsteady aerodynamic loads at the antenna locations,
- Aero-elastic research: to provide knowledge about amplitudes and frequencies of vibrations of the antenna surface and the surrounding aircraft structure due to unsteady aerodynamic loads,
- Structural dynamic research: to provide knowledge about the eigen-frequencies and

vibration modes of the unloaded aircraft structure (at locations of the antenna locations) and to provide knowledge about the magnitude of local steady displacements (due to steady aerodynamic loads).

- Avionics research: to provide knowledge about operational functions of conformal antennas, knowledge about requirements on possible antenna locations, knowledge about the modelling of conformal antennas, knowledge about effects of vibrations on performance of conformal antennas.

During the first period of the CLAAS project the computational modelling process has been described. An overview of this process is presented in figure 1. The process involves the specification of aircraft and antenna data, steady and unsteady aerodynamic calculations as well as electro-magnetic analysis of perturbed antenna surfaces. Furthermore, it was decided to apply the technology to a generic SAR antenna on the surface of a reconnaissance pod mounted at the centreline of a fighter aircraft. This location was selected because of the availability of finite element descriptions and because of the possibility to design a future demonstrator. An artist impression of the location of the antenna is displayed in figures 2 and 3. This generic SAR antenna is characterised by phased array antennas on two surfaces of the pod: one on the vertical side face of the pod and one on the lower face of the pod. The antennas on one side face and on the lower face are used to design a side-looking SAR antenna in a prescribed direction.

The aim of the present paper is to describe the technology development and to apply the technology to a generic phased array antenna on a faceted pod. The vibration modes of the front part of an unloaded reconnaissance pod have been computed. This knowledge is used to prescribe deformations of the antenna surface. The effects of deformation on the radiation pattern are investigated. The computational model for the determination of the disturbed radiation pattern is based on geometrical parameterisation of the Stratton-Chu integral equations.

AIRCRAFT DYNAMICS

Through the years the analysis of the dynamics of aircraft has been based on separate calculation of vibration characteristics of the aircraft structure and unsteady airloads. The vibration modes and reduced frequencies are computed by means of elasto-mechanical modelling. The unsteady airloads are then calculated for a range of reduced frequencies and vibration modes by unsteady aerodynamic analysis methods. Subsequently, the deformation of the aircraft structure (i.e. the amplitudes) is computed by combining the vibration modes and the unsteady airloads for representative flight conditions (e.g. a gust input). The generalised modal deflection system of the aircraft structure relates the amplitudes of the vibration modes to the unsteady dynamic loads. This approach implies that only the relevant flexible vibration modes have to be incorporated in the calculation of the deformation of the aircraft structure.

Elasto-mechanical modelling

As a representative test case the vibration characteristics of a fighter aircraft are discussed. The elasto-mechanical calculations require the availability of structural finite element data of the aircraft as well as computational methods. For the aircraft the vibration modes are distinguished for global modes (related to low frequency oscillations) and local modes (related to high frequency oscillations). This is illustrated in figures 4 and 5, where a conformal antenna is mounted on the upper side of a wing of a fighter aircraft. For low frequency oscillations the deformation of the aircraft structure is mainly governed by global vibration modes. In this case the displacement of the panel of the conformal antenna is nearly rigid and the mutual positions of the patches of the antenna do not change (see figure 4). On the other hand, for high frequency oscillations the deformation of part of the aircraft structure (e.g. the location of the conformal antenna) is mainly described by local vibration modes. In this case the panel is subject to a flexible motion and the mutual positions of the patches will change during a cycle of oscillation (see figure 5).

For the computation of the global vibration modes a structural model is required of the relevant part of the aircraft (e.g. fuselage, wing or vertical tail), where many details of the structure are not taken into account. However, for the computation of local vibration modes a more detailed model is required for a part of the aircraft structure where the antenna will be located. In this case, the finite element model should at least include the mass and stiffness properties of the spars, stiffeners and the skin plate. This is illustrated in figure 6, where the local finite element model of the front part of the reconnaissance pod is displayed. Figure 7 shows the computed vibration modes corresponding to an eigen-frequency of 442 Hz.

Unsteady aerodynamic analysis

The prediction of airloads on oscillating aircraft structures in subsonic and transonic flow requires the application of unsteady aerodynamic computational methods. Such methods are being developed at NLR since the seventies. For relatively high frequency oscillations, local unsteady airloads can be calculated by means of so-called piston theory. This theory is based on a local relation (i.e. locally at the antenna surface) between pressure and normal component of the fluid velocity. A computational method based on piston theory is developed in the framework of the CLAAS project. The aero-elastic analysis requires that the static and dynamic deformations of the aircraft geometry are determined, subject to aerodynamic and external forces acting on the aircraft. The geometrical state of the aircraft can be described by means of the superposition of the jig shape (i.e. the shape of the aircraft in unloaded state), the deformation due to steady aerodynamic forces (i.e. the change from the jig shape to the design shape under cruise conditions) and the dynamic deformations which are related to displacements belonging to some prescribed vibration modes. The amplitudes of the external forces are usually prescribed in relation to representative flight conditions.

Computation of dynamic deformations

It is assumed that the dynamic deformations can be described by a linear combination of a selected set of vibration modes, which are

denoted by $\vec{\phi}_v$, $v = 1, \dots, N$. The dynamic displacement \vec{d} can then be approximated by

$$\vec{d} = \sum_{v=1}^N q_v \vec{\phi}_v \quad (1)$$

The coefficients q_v are known as the generalised co-ordinates of the vibration modes. The values of q_v follow from the solution of the generalised modal deflection system which reads

$$M \frac{d^2 \vec{q}}{dt^2} + D \frac{d\vec{q}}{dt} + K\vec{q} = \vec{F}_a + \vec{F}_e \quad (2)$$

The matrices M , D and K are the generalised mass, damping and stiffness matrices, which result from the elasto-mechanical modelling. These matrices are related to the selected set of vibration modes. Furthermore, \vec{F}_a denotes the generalised aerodynamic force. Preliminary research has shown that piston theory yields an additional contribution to the damping and stiffness matrices. Furthermore, \vec{F}_e denotes a prescribed external force, which is typical for representative flight conditions. The basis of vibration modes $\vec{\phi}_v$ can be defined by a set of global or by a set of local vibration modes. The actual choice depends on the relevant part of the aircraft surface to be analysed. For the front part of the reconnaissance pod one of the local vibration modes is displayed in figure 7.

The above approach of computational modelling implies that aerodynamic and structural finite element data is available. Since NLR has data available of some fighter aircraft, the technology of the CLAAS project will be mainly applied to this type of aircraft. When these data would be available for other platforms (e.g. other aircraft, UAV's) the technology can also be used for the analysis of conformal antennas on these platforms.

Electro-magnetic modelling

The radiated electric field can be determined by the application of the Stratton-Chu integral representation formulas. The geometrical deformation of the antenna surface can be modelled in these formulas by introducing a geometrical parameterisation of the antenna

surface. The boundary points of the undisturbed antenna surface S_0 are assumed to be described by a map Ψ_0 , which maps a square reference domain Ω onto S_0 . The boundary points of the displacement \vec{d} (see equation 1) are defined by a similar mapping.

Then, the deformed antenna surface S_1 can be described by

$$\vec{\Psi}_1(\vec{u}) = \vec{\Psi}_0(\vec{u}) + \vec{d}(\vec{u}) \quad (3)$$

with $\vec{u} \in \Omega$

This is illustrated below for a vibration mode of a flat panel. Let the domain Ω be defined by the square rectangular domain $[-1, 1] \otimes [-1, 1]$. The points of a steady flat panel with length a and height b follow from the map

$$\vec{\Psi}_0(\vec{u}) = \vec{\Psi}_0^c + u_1 \frac{a}{2} \vec{\tau}_1 + u_2 \frac{a}{2} \vec{\tau}_2 \quad (4)$$

where $\vec{\Psi}_0^c$ denotes the centre point of the flat panel and $\vec{\tau}_1, \vec{\tau}_2$ orthogonal tangential vectors in the length and height direction, respectively. For small displacements the vibration modes of simply supported panels are given by

$$\vec{\phi}_{l,m}(\vec{u}) = \hat{n}_0 \sin(l\pi(u_1 + 1)/2) \sin(m\pi(u_2 + 1)/2) \quad (5)$$

where \hat{n}_0 is the normal vector of the undeformed flat panel. For increasing wave numbers of l and m these vibration modes have a more and more oscillatory character. In this paper the effects of deformation of the antenna surface on the radiation pattern are investigated for some representative vibration modes with prescribed amplitude. Then, the deformation \vec{d} is given by $\vec{d}(\vec{u}) = \alpha \vec{\phi}_{l,m}(\vec{u})$, with α prescribed. Then equation (3) reads

$$\vec{\Psi}_1(\vec{u}) = \vec{\Psi}_0(\vec{u}) + \alpha \vec{\phi}_{l,m}(\vec{u}) \quad (6)$$

The surface current distribution on the phased array antenna is assumed to be given by prescribed magnetic surface currents along the edges of the radiating patches (i.e. radiating slots) as described in [1], pp. 48-50. In the far field the radiated electric field due to radiating patches on

antenna surface S can be approximated by (see [2], pp. 87-88):

$$\vec{E}(\vec{r}) = -jk \frac{e^{-jkR}}{4\pi R} \int_S \vec{M}(\vec{r}') \times \hat{R} e^{jk\vec{r}' \cdot \hat{R}} ds' \quad (7)$$

where R is the distance from the origin to the observer and \hat{R} the unit direction vector from the origin to the observer. For the undeformed antenna the surface S is given by S_0 , while the perturbed antenna surface is given by S_1 . Thus, the deformation of the surface of the antenna is modelled in the formula for the electric field by introducing the map $\vec{\Psi}_1$ in the integral of equation (7). This formula assumes that the magnetic surface current \vec{M} is tangential to the surface S .

Numerical approach

The magnetic surface currents \vec{M}_0 on the undeformed surface are taken piecewise constant on the narrow slots along the radiating edges, while they are assumed to be zero elsewhere. The radiating slots are assumed to be aligned in the flight direction (i.e. the \hat{x} -direction), so that $\vec{M}_0 = M\hat{x}$. The patches of the antenna array are assumed to be locally planar on the deformed surface S_1 . Let \hat{n} be the normal vector at some patch and let \vec{a}_1, \vec{a}_2 be a local tangential base. In the application below, this local base is defined by the unitary vectors $\vec{a}_1 = \hat{x} \times \hat{n}$, $\vec{a}_2 = \hat{n} \times \vec{a}_1$, with \hat{x} the unit vector in flight direction. It can be shown that the magnetic currents on the perturbed surface follow from $\vec{M}_1 = M\vec{a}_2$. The normal vector \hat{n} can be computed by means of equation (6) (see [3]). In general, \vec{a}_1, \vec{a}_2 and \hat{n} will depend on α . As a consequence of this approach, the integral in (7) reduces to the summation of the sub-integrals over the slots of the separate patches. Hence (7) can be rewritten as

$$\vec{E}(\vec{r}) = -jk \frac{e^{-jkR}}{4\pi R} \sum_p (\vec{M}_{1,p} \times \hat{R}) \int_{A_p} e^{jk\vec{r}' \cdot \hat{R}} ds' \quad (8)$$

with p the index for patch number p . Furthermore, A_p denotes the united area of the

two radiating slots of patch number p . The phase integral in (8) can be computed in closed form by replacing the vector \vec{r}' by $\vec{r}^\bullet + \vec{a}_1\xi + \vec{a}_2\eta$, with \vec{r}^\bullet the centre of the radiating slots.

EXAMPLE OF AN AIRBORNE CONFORMAL ANTENNA

The effects of vibrations and deformations on the antenna performance were calculated for the case of a C-band SAR antenna on a pod attached to an aircraft. The antenna consists of a faceted two-dimensional conformal array of patch antennas. The number of antenna elements along-track will usually be higher than the number across-track because of the beamwidth requirements. Along-track, the array on the pod can be planar. However, across-track there may be a need for a conformal antenna on the curved surface of the pod. In this paper the deterioration of the antenna performance will be considered. Across-track a total beamwidth of approx. 12° was assumed, along track the beamwidth is approximately 8° . Sidelobe levels were set to a level below -20 dB. The array across-track consists of 2x8 patch antennas (8 patches on the lower side and 8 patches on the right side of the pod). The array length along-track is 24 elements. For this example the beam elevation was 45° w.r.t. nadir (see figures 8 and 9, $\theta=0^\circ$ is towards zenith, the ϕ -plane is the horizontal plane with $\phi=0^\circ$ being the flight direction). A potential deformation of the geometry is shown in figure 10. For this example, the effects of vibration levels with a maximum of $1/8$ lambda (approximately 6 mm) are shown in figures 11, 12 and 13. It can be concluded that for this level of vibration the radiation pattern is influenced significantly. In general, the side lobe level of a SAR antenna towards nadir ($\theta=90^\circ$) should be minimized to prevent strong reflections from the surface of the earth at normal incidence. Figure 13 shows that the sidelobe levels of the deformed antenna towards nadir may increase due to these deformations. The differences in the influence on the radiation pattern due to a symmetrical or due to an a-symmetrical deformation are also visible.

EXAMPLE OF A SPACEBORNE CONFORMAL ANTENNA

Part of the technology for airborne conformal antennas can also be applied to spaceborne antennas, where the deformation of the antenna surface may be due to thermal effects. The deformation of the surface can again be described by means of equation (1). However, there is no contribution of aerodynamic forces (i.e. $\vec{F}_a=0$) and the external force \vec{F}_e is related to thermal heating. The computation of vibration modes, eigen-frequencies and generalised mass, damping and stiffness matrices can be performed in a similar way as for airborne antennas. The effects of surface deformation of the antenna radiation pattern are shown in figures 14 and 15 for a case study of a spaceborne SAR antenna (frequency 6.6 GHz, wavelength 4.5 cm). This antenna consists of 60 times 20 radiating rectangular patches (size 1.5 cm times 1.5 cm, spacing between the patches 0.9 cm) on a flat plate. The size of the plate is 1.5 meter width and 0.5 meter height. The effects of surface deformation are shown for one vibration mode, which is displayed in figure 14. The vibration mode is given by equation (4) with $l=2$, $m=0$. The amplitude of the vibration mode is taken equal to λ (i.e. amplitude =4.5 cm). The disturbed radiation pattern is displayed in figure 15. For this vibration mode the effects on the radiation pattern are very clear: a shift of the main lobe as well as a change in side lobe level is observed.

POTENTIAL MEASURES TO REDUCE DEFORMATION AND VIBRATION EFFECTS

NLR has initiated research activities to reduce the effects of vibration. These activities are related to two topics: vibration suppression and electric compensation. Vibration suppression may be achieved by active devices as piezoelectric materials (actuators or thin layers) and intelligent control. A simulation tool (based on finite element technology) is being developed which takes into account modelling of piezoelectric devices and optimisation of their control voltages. Electric compensation may be achieved by adaptive digital beamforming. Here the

weights (amplitudes and phases) are adapted to the actual deformation. This requires an estimate of the excited vibration mode (frequency and amplitude) by means of passive sensors (e.g. accelerometers, strain gauges or micro electric-mechanical sensors) as well as the synthesis of appropriate weights, which are related to the intermediate stages of the antenna surface.

CONCLUSIONS

It can be concluded that the vibrations and deformations due to aerodynamic loads may have a significant influence on the performance of load-bearing antennas. Especially the changes in the antenna radiation pattern (beamwidth and sidelobe level) may have an adverse affect on the performance of a Synthetic Aperture Radar. The CLAAS project is an ongoing project. In the near future the effects of local unsteady airloads on actual vibration levels will be determined for a number of locations on the skin of a generic fighter aircraft. In addition the feasibility of compensation techniques has to be considered. Once these items are adequately covered, this technology may be applied to future SAR antennas at other non-conventional locations on the aircraft.

REFERENCES

- [1] I.J. Bahl, P. Bhartia, "Microstrip Antennas", Artech House, 1980
- [2] S. Silver, "Microwave Antenna Theory and Design", Peter Peregrinus, 1984
- [3] H. Schippers, F. Klinker, "Analysis of Conformal Antennas on Aircraft Structures", National Aerospace Laboratory NLR, TP99066, 1999

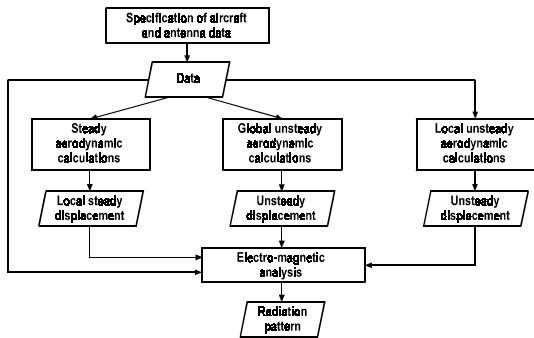
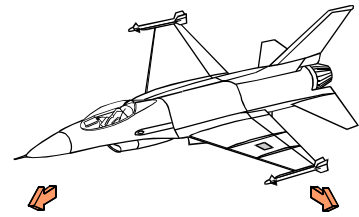
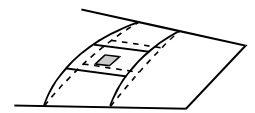
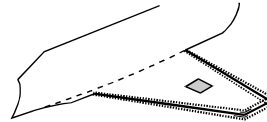


Figure 1 Overview of the computation modelling process



- Low frequency oscillations
- High frequency oscillation



- Global vibration modes
- Local vibration modes

Figure 4 Elasto-mechanical modelling of aircraft for analysis of conformal antennas

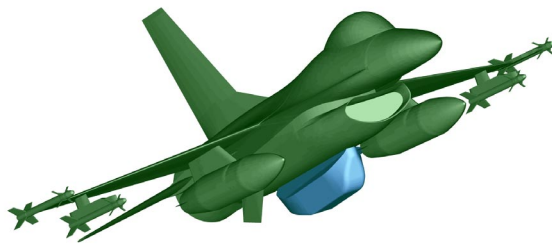


Figure 2 Fighter aircraft with reconnaissance pod

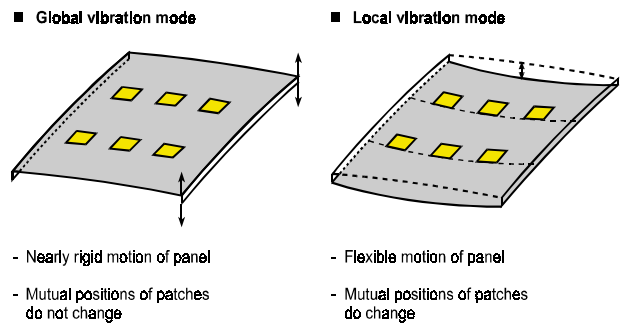


Figure 5 Global and local vibration mode

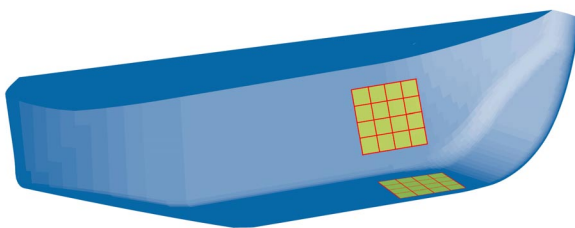


Figure 3 Artist impression of conformal antenna on a reconnaissance pod

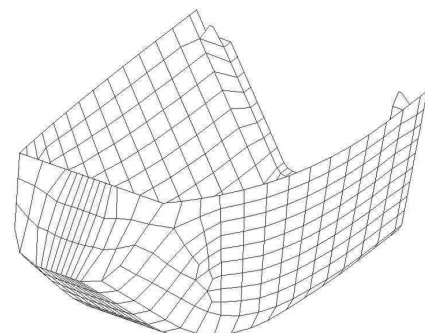


Figure 6 Finite Element model of the front of the reconnaissance pod



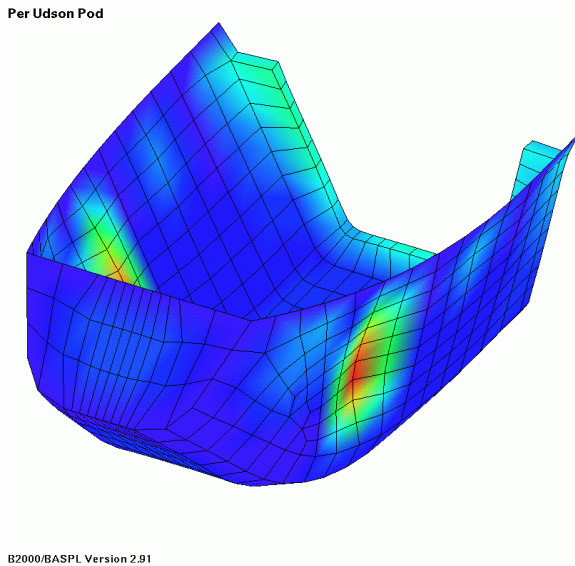


Figure 7 Vibration modes for an eigen-frequency of 442 Hz.

Figure 9. Across-track radiation pattern (non-deformed)

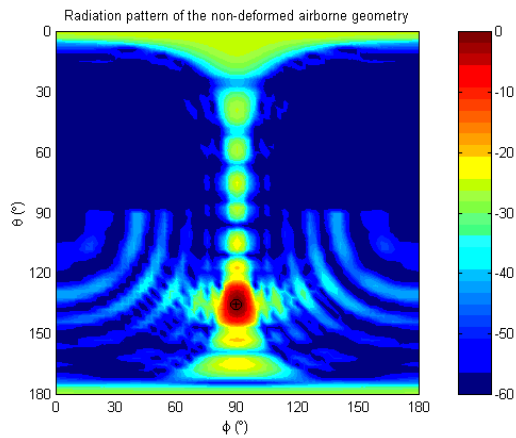
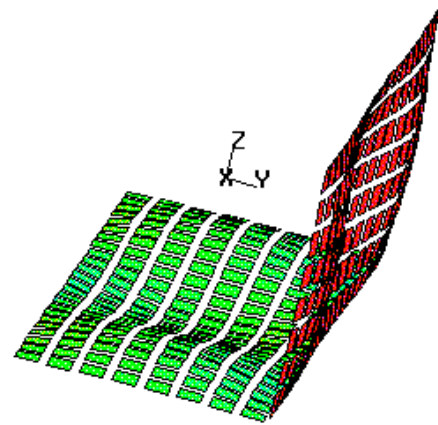


Figure 8 Radiation pattern of non-deformed geometry

Figure 10. Deformed geometry ($l=1, m=3$)

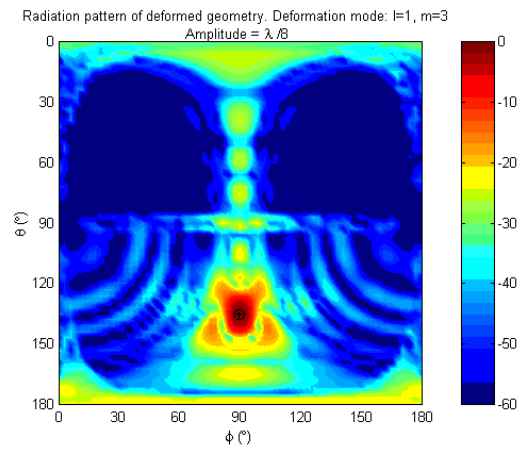
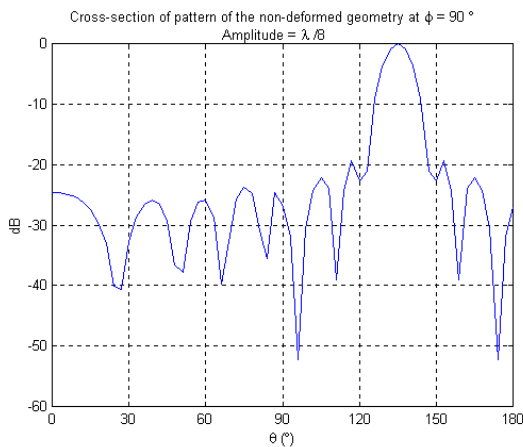


Figure 11 Symmetric deformation ($l=1, m=3$)



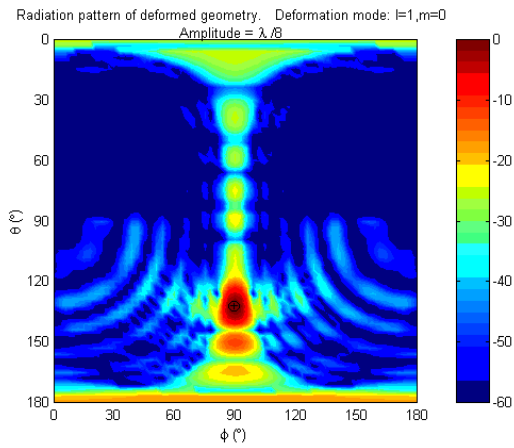


Figure 12 A-symmetric deformation ($l=1, m=0$)

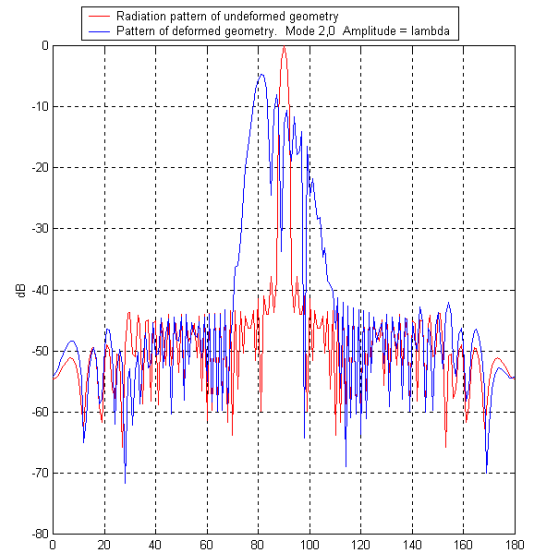


Figure 15 Radiation pattern deformed spaceborne SAR-antenna

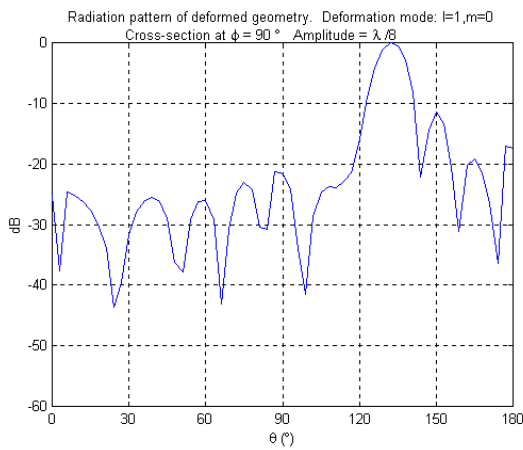


Figure 13. Across-track radiation pattern (a-symmetric deformation $l=1, m=0$)

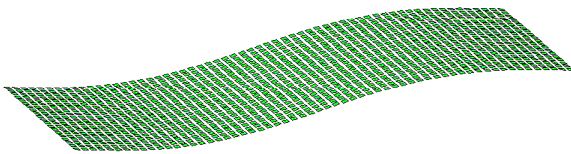


Figure 14 Deformed spaceborne SAR-antenna